



## ORIGINAL ARTICLE

# Graphene oxide modified glassy carbon electrode for determination of linagliptin in dosage form, biological fluids, and rats' feces using square wave voltammetry



Ahmed M. Hareedy<sup>a</sup>, Sayed M. Derayea<sup>b</sup>, Ahmed A. Gahlan<sup>c</sup>,  
Mahmoud A. Omar<sup>b,e</sup>, Gamal A. Saleh<sup>a,d</sup>

<sup>a</sup> Pharmaceutical Analytical Chemistry Department, Faculty of Pharmacy, Merit University, New Sohag, Egypt

<sup>b</sup> Analytical Chemistry Department, Faculty of Pharmacy, Minia University, Minia, Egypt

<sup>c</sup> Chemistry Department, Faculty of Science, Al-Azhar University, Assiut, Egypt

<sup>d</sup> Pharmaceutical Analytical Chemistry Department, Faculty of Pharmacy, Assiut University, Assiut, Egypt

<sup>e</sup> Pharmacognosy and Pharmaceutical Chemistry Department, College of Pharmacy, Taibah University, Medinah, Kingdom of Saudi Arabia

Received 19 October 2021; accepted 19 December 2021

Available online 23 December 2021

## KEYWORDS

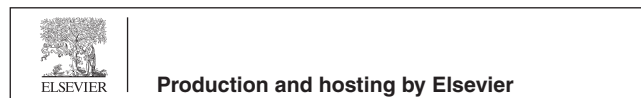
Square-wave voltammetry;  
Linagliptin;  
Graphene oxide modified  
glassy carbon electrode;  
Human biological fluids;  
Rats' Feces

**Abstract** An applicable square wave anodic adsorptive stripping voltammetric (SWAdASV) technique was utilized for linagliptin determination. A glassy carbon electrode was modified with graphene oxide to increase the electrode reactivity. The method is cheap, accurate, precise, and selective, with a good linearity range and a low detection limit. The proposed method was the first one to determine linagliptin in the feces, which is the main route for excreting the drug from the body. The electrode was characterized using various techniques, including Scanning Electron Microscope (SEM), Fourier-transform infrared (FTIR), and X-ray powder diffraction (XRD), and the oxidation mechanism of the drug was examined. The proposed method has a linear range of 9.45–103.96 ng mL<sup>-1</sup>. The detection limit was 4.0 ng mL<sup>-1</sup>. The modified electrode was employed efficiently to determine the drug in tablet formulations, spiked human urine, plasma, and rats' feces with high recoveries. The proposed method's results were statistically compared with those of another previously published method.

© 2022 The Authors. Published by Elsevier B.V. on behalf of King Saud University. This is an open access article under the CC BY-NC-ND license (<http://creativecommons.org/licenses/by-nc-nd/4.0/>).

E-mail address: [ahmed.mgahd@merit.edu.eg](mailto:ahmed.mgahd@merit.edu.eg) (A.M. Hareedy)

Peer review under responsibility of King Saud University.

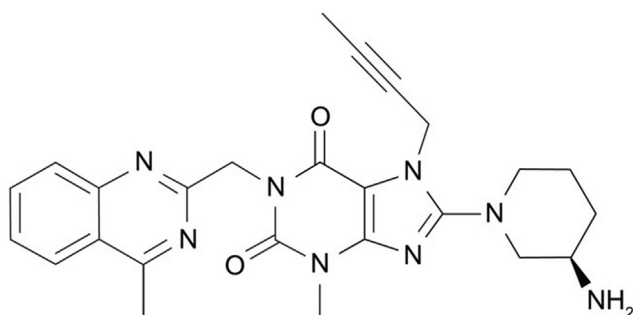


## 1. Introduction

Diabetes is a commonly dispersed and chronic disease worldwide. Approximately 5.1% of adults suffer from this disease (Bjornar et al., 2015). Nineteen million adults in Africa have

diabetes in 2020, 95% of which are type 2 and are estimated to grow to forty-seven million by 2045 unless controlled. In 2017, diabetes affected 451 million adults worldwide up from 138 million in 1980 and is expected to reach 600 million by 2045. Diabetes is a commonly dispersed and chronic disease worldwide. Approximately 5.1% of adults suffer from this disease (Bjørnar et al., 2015). Nineteen million adults in Africa have diabetes in 2020, 95% of which are type 2 and are estimated to grow to forty-seven million by 2045 unless controlled. Diabetes affects 451 million adults worldwide in 2017, up from 138 million in 1980, and is expected to reach 600 million by 2045 (Godman et al., 2020). Dipeptidyl peptidase-4 (DPP-4) inhibitors are among the newest categories of drugs used to treat type 2 diabetes. Their anti-hyperglycemic effect prevents the degradation of the incretin hormone, an intestinal peptide hormone secreted upon food intake, and improves the functions of pancreatic islets (Deacon, 2018). Dipeptidyl peptidase-4 (DPP-4) inhibitors are among the newest categories of drugs used to treat type 2 diabetes. Their anti-hyperglycemic effect prevents the degradation of the incretin hormone, an intestinal peptide hormone secreted upon food intake, and improves the functions of pancreatic islets (Deacon, 2018).

Linagliptin (LNG, scheme 1), approved by the FDA on May 2, 2011, is considered the most potent agent of DPP-4 inhibitors. It can be used alone or with other oral anti-hyperglycaemic drugs. LNG is excreted mainly unchanged via the feces (84.7%) and urine (5.4%) (Deeks, 2012). Until this paper's writing, there was no official method for determining LNG in any pharmacopeia (Rizk, 2020). However, there are a lot of methods reported to determine LNG either alone or with other antidiabetic drugs, such as; spectrophotometric (Patil and Patil, 2020; Aref et al., 2020; Vijayalakshmi and Naveena, 2019), spectrofluorimetric (El-Bagary et al., 2014; Aref et al., 2020; Omar et al., 2019; Elmasry, 2021); high-performance thin-layer chromatographic (Rizk, 2020; Patel, 2020; Bhole, 2017); high-performance liquid chromatographic (Bhole et al., 2017; Sivagami et al., 2020; Raut et al., 2020; Kiran et al., 2020); conductometric (Al-Bratty and H, Almanaa, A. Tawhari, M.Q. Rehman, Z. U. Alhazmi, H. A. Javed, S. A. Alam, and Md. S., , 2019) and voltammetric (Elshahed et al., 2020; Naggar et al., 2020; Gahlan, 2021; Ateş et al., 2021; Gahlan, 2021; El-Shal et al., 2019; Baezzat and Shojaei, 2021) methods. Some of these methods are shown in Table 1. Additionally, some of these methods have sufficient limits of quantification and detection. However, most of these methods are time-consuming, costly, and require a complex sample pre-treatment process.



Scheme 1 LNG chemical structure.

**Table 1** Some of the reported methods were used to determine LNG.

The method	LOD (ng ml-1)	Ref.
Zero-order UV Spectrophotometry method	82.0	(Patil and P. a., 2020)
spectrofluorometric method	79.0	(Omar et al., 2019)
HPTLC	100.0	(Bhole, 2017)
HPLC	20.0	(Kiran et al., 2020)
Conductometry	3544.0	(Al-Bratty and H, Almanaa, A. Tawhari, M.Q. Rehman, Z. U. Alhazmi, H. A. Javed, S. A. Alam, and Md. S., 2019)
Voltammetry	52.0	(Gahlan, 2021)

Electrochemical methods have been widely employed in the last decade to determine pharmaceutical agents because they are inexpensive, simple, quick, and can be used in different biological samples (Yang et al., 2015). One of the highly sensitive electrochemical methods for analytical applications is square-wave voltammetry (SWV) because it combines the advantages of cyclic voltammetry, impedance, and pulse techniques (Mirceski et al., 2013).

Glassy carbon electrode (GCE) is a relatively pure material, highly inert to chemical attack, gas impermeable, electrically conductive, and easily modified (Shigemitsu et al., 1979).

Carbon-based compounds are commonly used because of their biocompatibility, good chemical stability, high surface area, unique electrical properties, good electron transfer kinetics, and low cost (Yang et al., 2015). Graphene oxide has a high capacitance, probably due to its oxygen-containing functional groups on the surface because it has an extended aromatic lattice of graphene containing ketone carbonyls, epoxides, carboxylic groups, and alcohols (Marcano, 2010; Kariper et al., 2019; Korkmaz and Kariper, 2020). These functional groups allow for their reactions with different pharmaceutical drugs. These properties make it preferable to graphene as an electrode material (Korkmaz and Kariper, 2020). GCE modified with Go (GCE-GO) was used to determine some drugs like flutamide, salicylic acid, and paracetamol (Karthik, 2017; Vadivaambigai, 2015; Zidan, 2014).

Two techniques based on voltammetry were previously described for LNG determination utilizing an electrode of carbon paste (CPE) after its modification either with iron oxide nanoparticles (Fe<sub>2</sub>O<sub>3</sub>NPs) (El-Shal et al., 2019) or cobalt oxide nanoparticles (Co<sub>3</sub>O<sub>4</sub> NPs) linked to multiwall carbon nanotubes (Elshahed et al., 2020). However, CPE has many limitations because it needs a high level of experience in its use; each prepared unit may vary in the physicochemical and electrochemical characters, relative weaker fabrication reproducibility, low mechanical stability, and mechanical destruction that may happen upon usage (Canbay et al., 2014). The other reported voltammetric methods (Elshahed et al., 2020; Naggar et al., 2020; Gahlan, 2021; Ateş et al., 2021; Gahlan, 2021; El-Shal et al., 2019) for LNG determination are less sensitive than the cited one. Also, in the current method, a GCE-GO was used to determine LNG in the authentic, pharmaceutical preparation, spiked human urine,

and spiked human plasma. Moreover, it is the first method to determine LNG in the rats' feces.

## 2. Experimental

### 2.1. Apparatus

All square-wave voltammetry (SWV) and cyclic voltammetry (CV) measurements were performed using an EG & G Princeton Applied Research Model 273 potentiostat (PAR Princeton, NJ, USA) operated by 270/250 electrochemical software (Version 4.30). The unit was connected to a three-electrode system. The glassy carbon electrode (G0229 multi-electrode 2.0 mm manufactured by Princeton Applied Research, PAR Princeton, NJ, USA) modified with GO was used as the working electrode. The auxiliary electrode was a platinum wire. In contrast, the reference electrode was Ag/AgCl (saturated KCl). A magnetic stirrer, C-MAG HS 7 (IKA Labortechnik, Germany), with a Teflon-coated bar, was utilized to speed up the cell's mass transport. A JEOL Scanning Electron Microscope JSM-5410LV (JEOL, Ltd. Tokyo, Japan) was employed for morphological characterizations. A Nicolet™ iS10 Fourier-transform infrared (FTIR) spectrometer (Thermo Fisher Scientific, Massachusetts, USA) was used to characterize the function groups. The crystalline characteristics were examined using an X-ray powder diffraction (XRD) device, Bruker-AXS D4, produced by Sietronics Pty Ltd (Mitchell, Australia). The biological samples were prepared using a laboratory 12,000 RPM model PLC-012 centrifuge (Taiwan). All tests were conducted at room temperature ( $25\text{ }^{\circ}\text{C} \pm 2$ ) and without oxygen expelling. The pH was measured with an iMeshbean pH-108 IA pH Meter (China).

### 2.2. Reagents and materials

Graphite (fine powder, 98% pure, was purchased from Loba Chemical Pvt. Ltd. (Mumbai, India). Potassium permanganate, hydrogen peroxide (30%), methanol, disodium hydrogen phosphate, sodium dihydrogen phosphate, sodium hydroxide, boric acid, citric acid, glacial acetic acid, sulfuric acid, orthophosphoric acid, and hydrochloric acid were obtained from El-Nasr Chemical Company (Giza, Egypt). Analytical grade chemicals were used throughout the work.

Phosphate buffer, which consists of disodium hydrogen phosphate and sodium dihydrogen phosphate, was prepared daily in double-distilled water.

LNG, Batch No: AA4307BA, was generously supplied by RAMEDA (10th Ramadan, Cairo, Egypt). In addition, Trajenta® tablets (Boehringer Ingelheim, Germany), containing 5.0 mg of LNG per tablet, were brought from an Egyptian pharmacy.

The LNG stock solution ( $4.73\text{ mg mL}^{-1}$ ) was prepared by dissolving 47.30 mg of LNG in 10.0 mL of methanol, and it was kept in the fridge. Working solutions were prepared from the previous stock by dilution with distilled water.

### 2.3. Electrode preparation

GO was prepared according to the modified Hummer's method (Hummers and R. e., 1958). First, a beaker was

placed into an ice bath connected to a magnetic stirrer; 25.0 mL of  $\text{H}_2\text{SO}_4$ , 1.0 g of graphite powder, and 3.0 g of  $\text{KMnO}_4$  were added very slowly with caution. The temperature must be less than  $20\text{ }^{\circ}\text{C}$ , and the mixture must be stirred for three hours before adding 25.0 mL of distilled water dropwise and slowly to begin the oxidation process. Next, the solution color was transferred from black to dark brown, indicating the formation of GO. Instantly, 100.0 mL of distilled water was added to oxidize any lifted graphite. The reaction was then stopped by adding 5.0 mL of  $\text{H}_2\text{O}_2$  to interact with the excessively unreacted permanganates. Next, the GO formed was washed with 200.0 mL of distilled water, 200.0 mL of 30% HCl, 200.0 mL of methanol, and 200.0 mL of distilled water, respectively, in one wash cycle. After each addition, the GO was filtered. Finally, the formed GO was dried in an oven for 24 h at  $40\text{ }^{\circ}\text{C}$  and finally powdered using an electric grinder.

GCE was carefully polished with alumina powder, followed by sequential sonication in ethanol and distilled water. After the GCE surface was dried,  $4.0\text{ }\mu\text{L}$  of  $1.0\text{ mg mL}^{-1}$  watery GO solution was added to the GCE surface and left to dry for about 20 min at room temperature before running each electrochemical measurement.

### 2.4. Procedures

#### 2.4.1. General procedure for LNG determination in standard solutions

The modified GCE-GO was immersed in a 40 mM phosphate buffer (pH 6.5). Then, using SWAdASV, the solution of  $96.95\text{ ng mL}^{-1}$  LNG was stirred while applying the accumulating potential ( $+0.60\text{ V}$ ) versus the reference electrode (Ag/AgCl) for 480 s. After stopping the stirring, the solution was left for 10 s to be stagnant before running the voltammetric scan ( $+0.6\text{--}1.6\text{ V}$ ). Before that, a similar procedure was repeated in the absence of LNG.

#### 2.4.2. Pharmaceutical tablets analysis procedure

To get an LNG solution with a concentration of  $4.73\text{ mg mL}^{-1}$ , the specific weight of powdered ten Trajenta® tablets was calculated and weighed. Then, the powder was dissolved with 5.0 mL of methanol by sonication for 20 min in a 10.0 mL volumetric flask. After that, methanol was used to bring the solution volume up to volume. Following filtration, a portion of the LNG tablets stock solution was diluted with distilled water to obtain an LNG working solution at the desired concentration. Finally, the voltammetric measurement was done as mentioned before.

#### 2.4.3. Procedure for analysis of spiked human urine

A healthy volunteer's urine sample was subjected to centrifugation for 20 min at 3500 rpm. The supernatant was mixed with 1.0 mL of acetonitrile and centrifuged again for 20 min at 3500 rpm to precipitate the protein content efficiently. An aliquot of 1.50 mL of the resulting supernatant was added to an electrochemical cell, and the volume was totaled to 15.0 mL with a 40 mM phosphate buffer solution (pH 6.5). After adding the LNG working solution, whose concentrations were mentioned in Table 8, the voltammetric measurements were done as mentioned before.

#### 2.4.4. Procedure for spiked human plasma analysis

A healthy volunteer's plasma sample was subjected to centrifugation for 30 min at 4500 rpm. To efficiently precipitate the protein content, 0.5 mL of the supernatant was mixed with 1.0 mL of acetonitrile, and then 0.5 mL of 4.73 mg mL<sup>-1</sup> of LNG was added. Using distilled water, the volume was totaled to 5.0 mL and subjected to centrifugation for 30 min at 4500 rpm. As mentioned before, the voltammetric measurement was performed on a portion of the clear solution.

#### 2.4.5. Determination of LNG in rats' feces

The rats utilized were three healthy male Wistar Albinos weighing approximately 160.0 g. Rats were given LNG by oral gavage (2 mg/kg) after a 12-hour fast. First, a sample of 24-hour rat feces was collected, crushed, and stored at -4°C until use. Then, 0.5 g of this sample was transferred to a stoppered tube filled with methanol to a volume of 10.0 mL. Next, the content was centrifuged for 10 min at 4500.0 rpm. After that, the supernatant was mixed with 1.0 mL of acetonitrile and centrifuged again for 20 min at 3500 rpm to precipitate the protein content efficiently. Finally, the produced supernatant was treated using the conventional addition procedure, and the analysis was conducted as in the pure form section.

### 3. Result and discussion

#### 3.1. Characterization of graphene oxide

Scanning Electron Microscope (SEM), Fourier-Transform Infrared (FTIR), and X-ray Powder Diffraction (XRD) were used to characterize the prepared GO.

The comparison of Fig. 1(a) of graphite and (b) of GO by using an SEM scan shows an apparent morphological difference between them. The typical FTIR spectra for GO presented in Fig. 2 show the O-H band at 3383.94 cm<sup>-1</sup>, the aliphatic C-H band at 2925.55 cm<sup>-1</sup>, the C=O carboxy vibration at 1744.73 cm<sup>-1</sup>, the C=O band at 1537.14 cm<sup>-1</sup> and the C-O at 1382.00, 1219.26 cm<sup>-1</sup>, and 1046.10 cm<sup>-1</sup>, which is very close to the results obtained by Chaiyakun et al. (Chaiyakun et al., 2012). Fig. 3 shows the XRD patterns

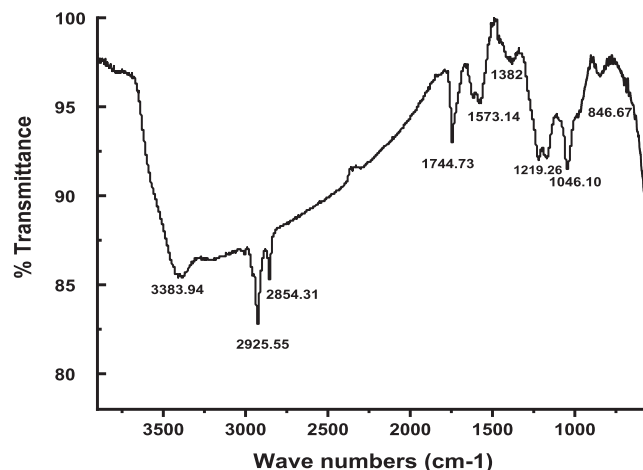


Fig. 2 FTIR spectra of the prepared graphene oxide (GO).

for GO with a sharp peak at 10.49° (8.43 Å), a peak at 21.08° (4.21 Å), and a peak at 26.45° (3.37 Å) which is close to the reported XRD spectra of GO (Bahrami et al., 2019; Albayrak, 2017).

#### 3.2. Surface morphology study of GO-GCE

After the modification of GCE with the prepared GO, SEM was used to evaluate the surface of the modified electrode. Fig. 4 shows the morphology difference between free GO-GCE and GO-GCE after the adsorption of LNG layers on its surface. By comparison, Fig. 4(a) and (b), the LNG was absorbed successfully on the surface of the electrode, which led to the change in the image morphology.

#### 3.3. Electrochemical behavior of LNG

The electrochemical behavior of LNG on GO-GCE was investigated using cyclic voltammetry. In a 40 mM phosphate buffer, LNG has one oxidation peak of + 1.06 V (pH 6.5). The

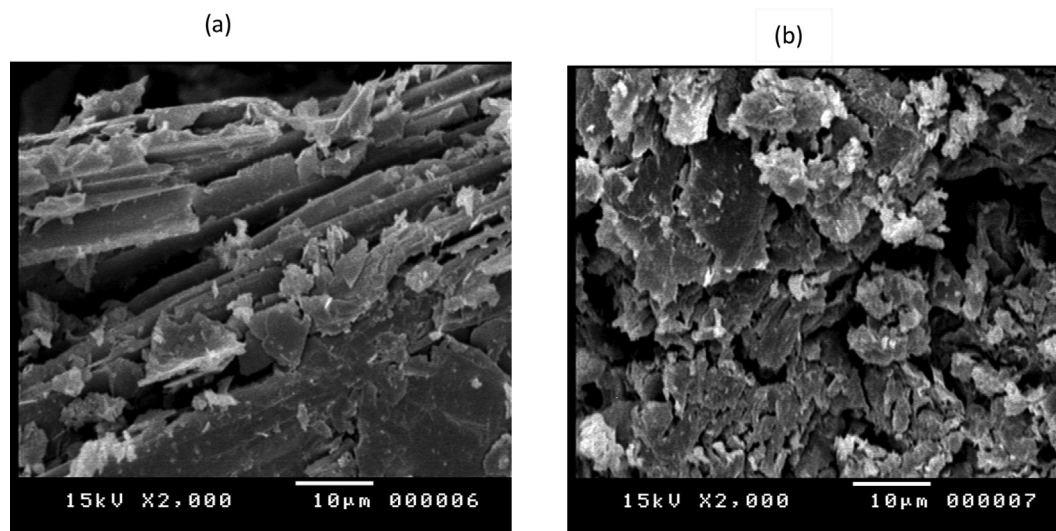
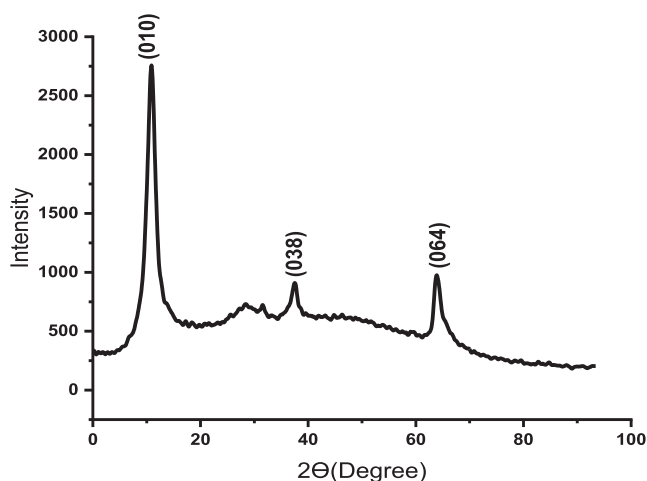


Fig. 1 Microphotographs of graphite (a) and graphene oxide (GO) (b) at one degree of magnification.



**Fig. 3** X-ray diffraction patterns of the prepared graphene oxide (GO).

reverse scan revealed no peak, indicating that LNG oxidation is irreversible. For further confirmation of the irreversibility of LNG oxidation, cyclic voltammetric scans for  $96.95 \text{ ng mL}^{-1}$  LNG were carried out at different speeds ranging from 0.1 to 1.0 V/sec. It was observed that the peak potential was shifted to a higher positive value by increasing the scan rate, as shown in Fig. 5 (a), supporting the hypothesis of non-reversible drug oxidation. The peak current is shown to be dependent on the scan rate square root (Fig. 5b). A linear relationship was observed, which can be expressed as follows:

$$I_p(\mu\text{A}) = 3.731v^{1/2}(\text{V}/\text{sec})^{1/2} + 0.9963(R^2 = 0.9986)$$

Based on these results, the oxidation of the drug is considered to be controlled by diffusion (Prashanth et al., 2011, 2011).

In addition, Fig. 5(c) depicts the dependence of the measured peak potential ( $E_p$ ) on the logarithmic scan rate ( $\log$ ). The obtained relationship was linear, which confirmed the mixed diffusion-adsorption nature of LNG oxidation. This result could be described using the following equation:

$$E_p = 0.1056 \text{Log}v(\text{V}/\text{sec}) + 1.1836(R^2 = 0.9941)$$

Given that LNG oxidation is an irreversible reaction, the correlation of the peak potential ( $E_p$ ) versus the logarithm of the scan rate ( $\text{Log}$ ) can be described by the Laviron equation (Laviron, 1979) as follows:

$$E_p = E^\circ + \left(\frac{2.303RT}{\alpha zF}\right) \text{Log}\left(\frac{RTK_s}{\alpha zF}\right) + \left(\frac{2.303RT}{\alpha zF}\right) \text{Log}v$$

Where  $E^\circ$  is the standard peak potential,  $v$  is the rate of the potential scan,  $K_s$  is the reaction rate constant,  $z$  is the number of electrons involved in the reaction,  $R$  is the gas constant,  $F$  is the Faraday constant, and  $T$  is the temperature in Kelvin. Then, the acquired slope can be used to compute the  $z$  value from the following formula: After fitting the values of  $\text{Log } v$  vs.  $E_p$ , as shown in Fig. 5 (d), the resulting slope can be used to determine the  $z$  value from the following formula:

$$\text{Slope} = \frac{2.303RT}{\alpha zF}$$

It was found that the value of the slope was 0.1056. From which,  $\alpha$  was estimated, and it was found that its value was equal to 0.51. If we assume that the value of  $\alpha$  is about 0.5, then the calculated value of the number of electrons ( $z$ ) involved in the reaction would be 1.12. This value proved that only one electron was involved in the oxidation of LNG (Naggar et al., 2020) (Scheme 2).

#### 3.4. Optimization of experimental parameters

After modifying a bare GCE using Go, SWAdASV was used to determine LNG (GO-GCE). Because of the increased surface area and unique electrical features of GO, the oxidation peak current of LNG improved upon modification with GO by about 18.34%, as shown in Fig. 6.

##### 3.4.1. Effect of buffer compositions

Five buffer solutions with different chemical compositions were studied, including Britton–Robinson, phosphate, citrate, citrate–phosphate, and Teorell–Stenhagen. According to Fig. 7, phosphate buffer produced the better oxidation peak

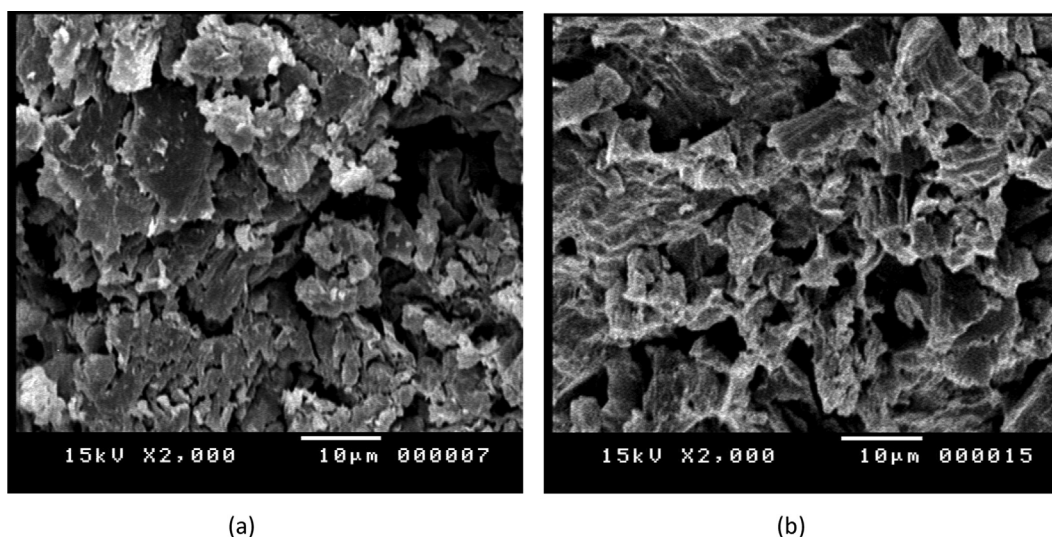
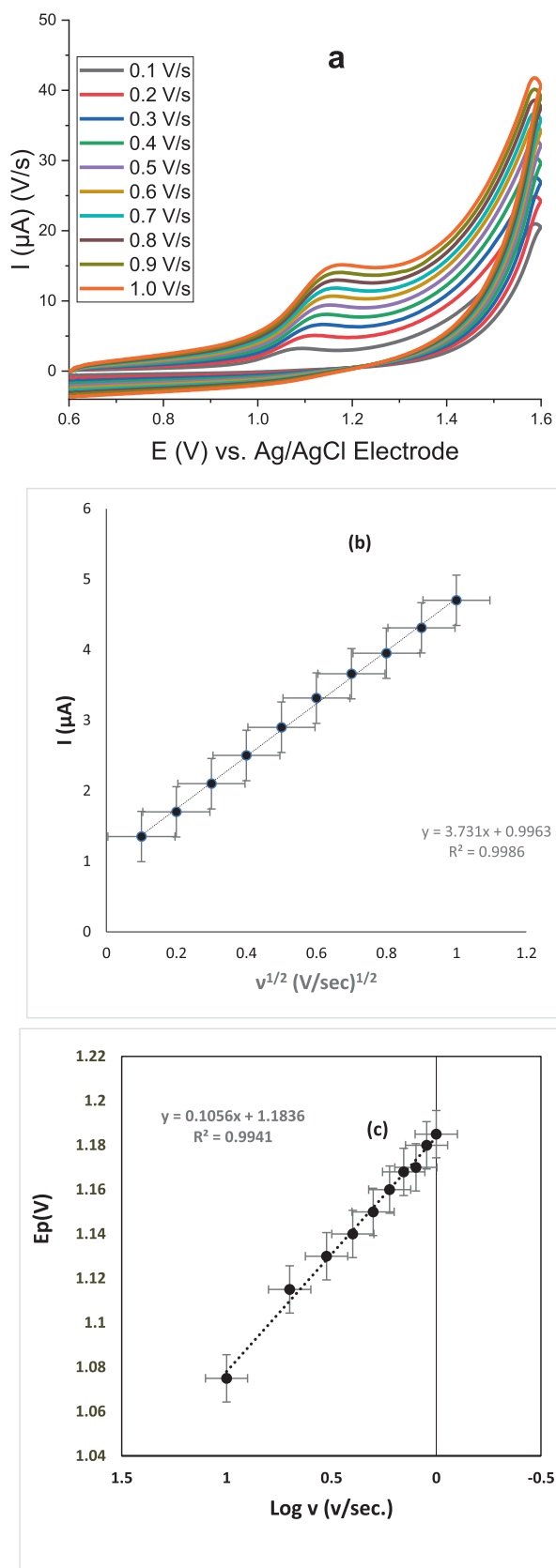


**Fig. 4** Microphotographs of Free GO-GCE (a) and GO-GCE of LNG layers (b) at one degree of magnification.



current, and so, it was used for subsequent studies. This result was due to the ionic mobility of phosphate, which is higher than the other used electrolytes (Kim, 2010).

### 3.4.2. Effect of pH and ionic strength

The pH and ionic strength of the selected buffer (phosphate buffer) solution were studied. The oxidation peak current was increased by increasing pH from 2.5 to 6.5 and reached its maximum value at 6.5. After that, as demonstrated in Fig. 8(a), increasing the pH causes a drop in the observed current. So, pH 6.5 was chosen for the method. At the same time, increasing pH values were also accompanied by a shift in the peak potential to low positive values (Fig. 8b, c). This behavior implies that the oxidation process involves electrons. The following equation describes the linear relationship between the measured peak potential and the pH values of the solution:

$$E_p = -0.055\text{pH} + 1.3968 (R^2 = 0.9806)$$

The nearness of the obtained value of the slope ( $-0.055 \text{ V/pH}$ ) in the previous equation to the theoretical value ( $-0.059 \text{ V/pH}$ ) means that one electron and one proton are involved in the electrode reaction during LNG oxidation (Gowda, 2014).

The influence of phosphate buffer concentrations on the oxidation peak current is also investigated, with the results reported in Fig. 8(d). The studied concentrations were 100, 80, 60, 40, 20, and 10 mM. It was found that 40 mM produced the highest oxidation peak current.

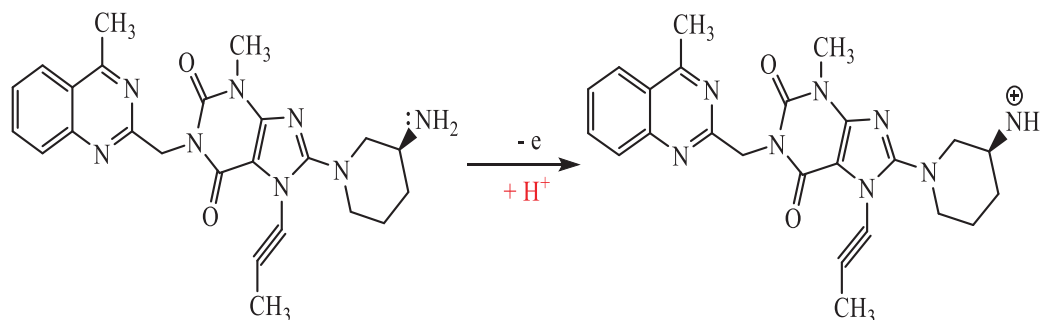
Some supporting electrolytes were also studied to enhance the peak current, such as KCl,  $\text{NaNO}_3$ , and  $\text{NaClO}_4$ . However, all these salts decreased rather than increased the peak oxidation current because they may have raised the Faradic responses that reacted with the intended product of the oxidation process or by their adsorption on the electrode surface and altered its kinetics (Allen and Larry, 2001).

### 3.4.3. Effect of GO concentration

Different concentrations of GO ( $0.1, 0.5, 1.0, 1.5,$  and  $2.0 \mu\text{g mL}^{-1}$ ) were studied. The recorded oxidizing peak currents were 21.01, 26.45, 32.53, 31.99, and  $31.36 \mu\text{A}$ , respectively. and volumes ( $1.0, 2.0, 4.0, 6.0, 8.0,$  and  $10.0 \mu\text{L}$  of  $1.0 \mu\text{g mL}^{-1}$ ) were applied to modify the GCE surface. The recorded oxidizing peak currents were 25.95, 30.39, 25.43, 22.16, 19.49, and  $18.54 \mu\text{A}$ , respectively. The best results were obtained when  $4.0 \mu\text{L}$  of  $1.0 \text{ g/mL}^{-1}$  GO solution was used.

So, the optimum experimental parameters for the proposed method were 40 mM phosphate buffer solution (pH 6.5), without salts as a supporting electrolyte, and with  $4.0 \mu\text{L}$  of  $1.0 \mu\text{g mL}^{-1}$  of GO solution.

**Fig. 5** (a) Typical cyclic voltammogram for  $96.95 \text{ ng mL}^{-1}$  LNG oxidation using GO-GCE at scan rate values (0.1–1 V/s), pH 6.5, accumulation potential + 0.6, and accumulation time 60 s. (b) The linear relationship shows the dependence of LNG oxidation peak current on the square root of studied scan rate values and (c) logarithm LNG peak current values.



**Scheme 2** The proposed oxidation mechanism of LNG.

#### 3.4.4. Effect of accumulation potential

The studied accumulation potential ( $E_{acc}$ ) was recorded in the range of (- 0.50 to + 1.00 V) (Fig. 9(a)). The oxidation peak current was increased using potentials ranging from - 0.50 to + 0.60 V, then remained constant up to + 0.90 V, before decreasing at higher potentials. Therefore, (+0.60 V) was used in the subsequent examinations as an accumulation potential.

#### 3.4.5. Effect of accumulation time

As shown in Fig. 9(b), the recorded oxidizing peak current was increased from 10 s by increasing the accumulation time up to 480 s, and then it was slightly decreased. This decrease happened because the surface of the GO-GCE became saturated with the adsorbed LNG.

Thus, the most optimum instrumental conditions for the oxidation of LNG on the surface of GO-GCE were + 0.60 V as accumulation potential and an accumulated time of 480 s.

#### 3.4.6. Effects of frequency, pulse amplitude, and scan increment

The effects of frequency (50–300 Hz), pulse amplitude (30–230 mV), and scan increment (1–5 mV) were also studied. Increasing the value of these three parameters is due to their impact on the capacitive current generation. This effect increases the peak current, but the curve is distorted at higher values, decreasing the sensitivity (Gopalan et al., 2007; Scholz, 2015; Teófilo et al., 2004).

In Fig. 10, the frequency was studied between 50 and 300 Hz. The maximum value of its conduct with the proposed method was 130 Hz. Second, the pulse amplitude was tested to choose the most suitable one for the cited method from 30 to 230 mV, which was 150 mV. Third, the scan increment was observed between 1 and 5 mV. Therefore, 3 mV was the chosen value.

Finally, the most optimum instrumental conditions to study the oxidation of LNG on the surface of GO-GCE were accumulation potential (+0.60 V), accumulated time (480 s), frequency (130 Hz), pulse height (150 mV), and scan increment (3 mV).

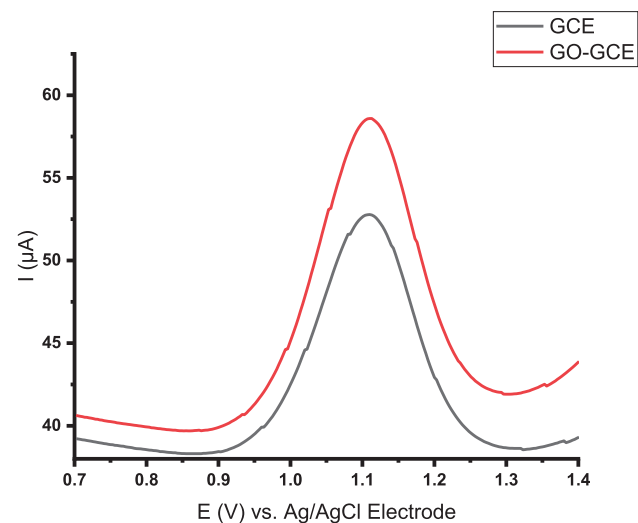


**Fig. 6** Square wave voltammogram of free GCE – LNG and after modification of GCE with graphene oxide (GO-GCE) in presence  $2.27 \mu\text{g mL}^{-1}$  LNG. Conditions; 0.04 M phosphate buffer (pH 6.5), accumulation potential + 0.6, and accumulation time 480 s.

### 3.5. Validation of the proposed method

The suggested method was assessed for linearity, range, detection and quantitation limits, precision, accuracy, and selectivity in compliance with the International Council for Harmonisation (Validation of analytical procedures: text and methodology Q2 (R1), 2005).

#### 3.5.1. Linearity and range

The proposed SWAdASV technique was used to determine a series of LNG standard solutions under the optimized conditions; 40 mM phosphate buffer (pH 6.5), accumulation time of 480 s, equilibrium time of 10 s. The accumulation potential was + 0.60 V, and the GO volume applied to the electrode surface was 4.0 L of  $1.0 \text{ g mL}^{-1}$ . The range within which LNG concentrations was related to voltammetric response was  $9.4 \text{--} 103.96 \text{ ng mL}^{-1}$ . Fig. 11 demonstrates the voltammograms and the calibration graph for different concentrations of LNG by the proposed method at the optimal experimental conditions. Table 2 shows the statistical results for the determination of LNG using GO-GCE. The correlation coefficient indicated that the method had a good linear response ( $R^2 = 0.9981$ ). The linear regression equation was  $y = 0.0493x + 12.222$ .

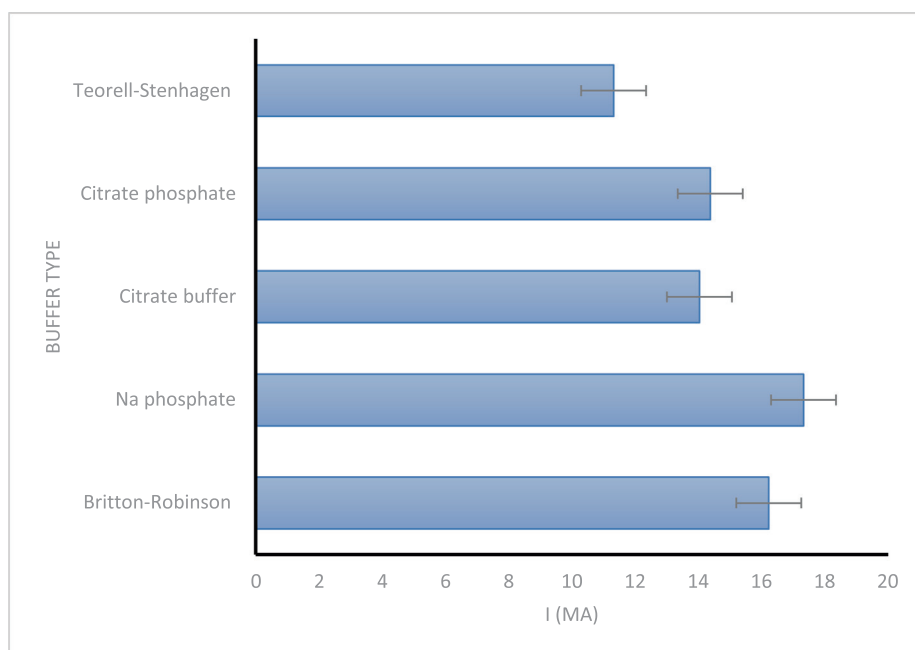


**Fig. 7** Effect of buffer type on the voltammetric peak current of  $96.95 \text{ ng mL}^{-1}$  LNG using different buffer types (pH 6.5) using GO-GCE modified (Accumulation potential + 0.6, accumulation time 60 s.)

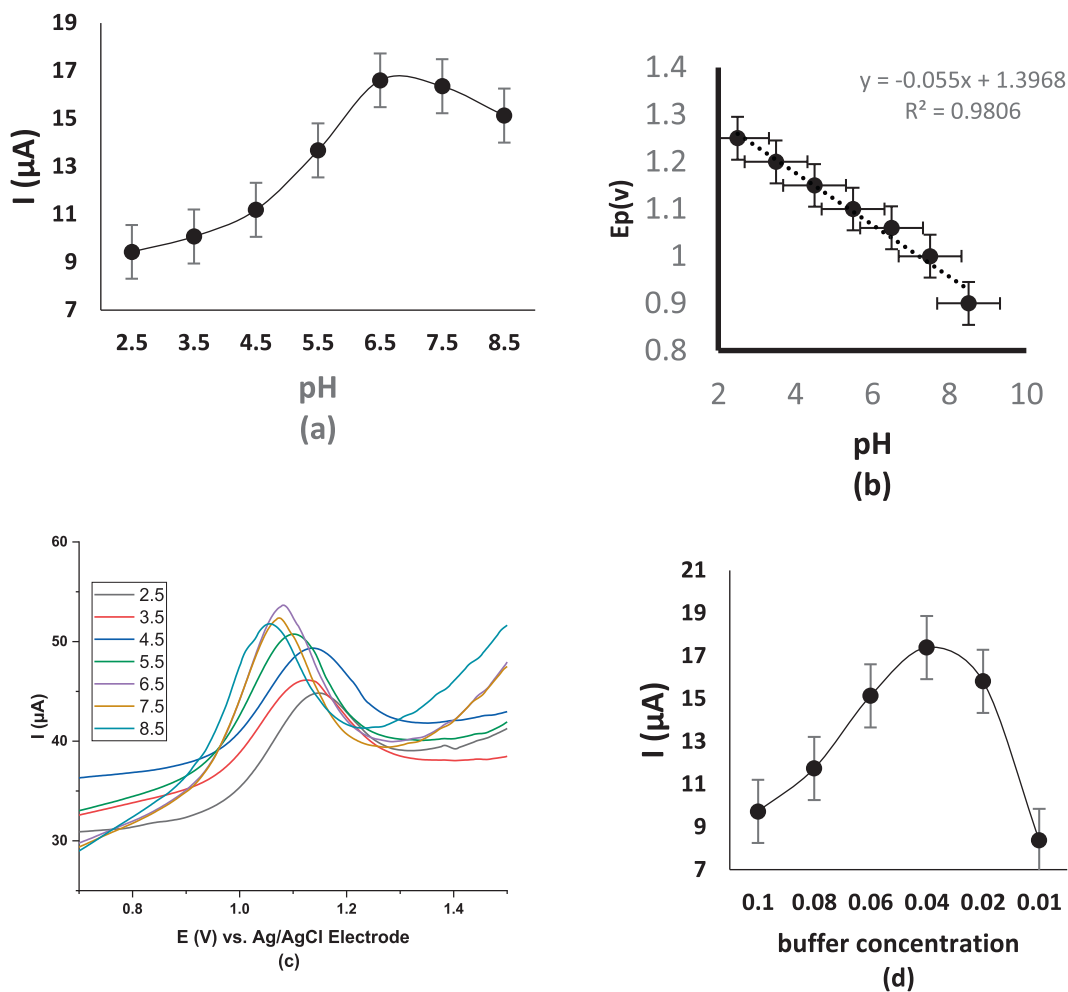


**Fig. 8** (a) Effect of pH, (b) Linear relationship of pH and the square root of the studded scan rate values, (c) pH voltammograms, and (d) phosphate buffer concentration on the peak current of  $96.95 \text{ ng mL}^{-1}$  LNG on GO-GCE (accumulation time 60 s.)

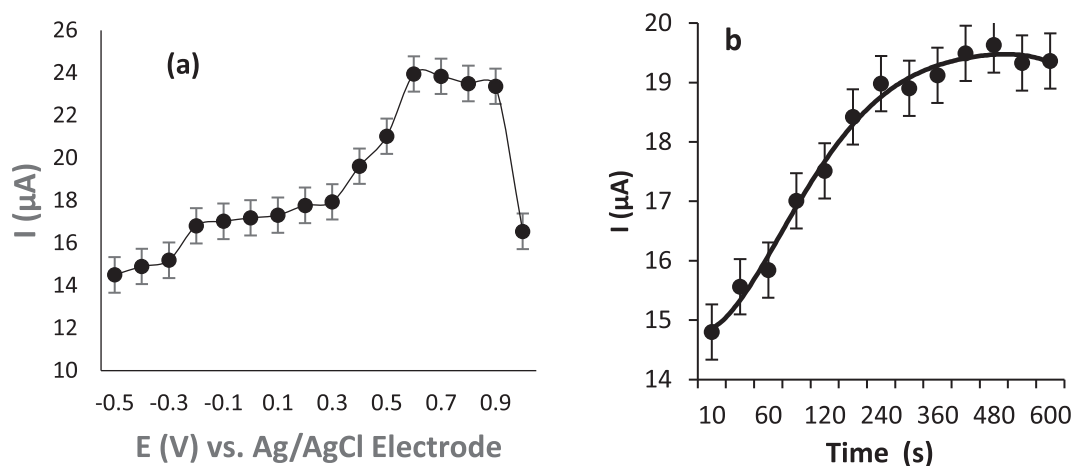


**Fig. 9** (a) Plot of the peak current of  $96.95 \text{ ng mL}^{-1}$  LNG at different accumulation potentials (V) accumulation time 60 s. (b) The relationship between  $I_p$  peak current and accumulation time (s).

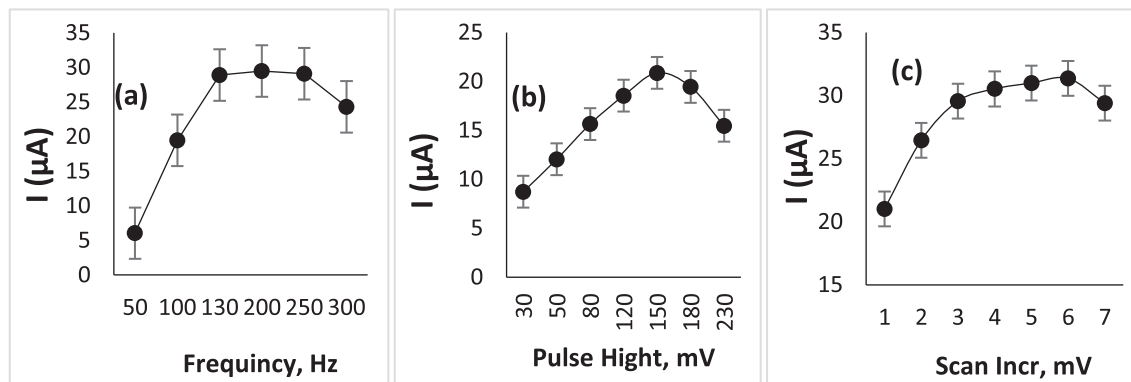


**Fig. 10** (a) Effect of Frequency, (b) Pulse Height and scan increment on the peak current of  $96.95 \text{ ng mL}^{-1}$  LNG on GO-GCE (accumulation time 60 s.)

### 3.5.2. Detection and quantification limits

Detection (LOD) and quantification (LOQ) limits were estimated using the following formula:  $LOQ = 10\sigma/S$  and  $LOD = 3\sigma/S$ .  $S$  represents the calibration curve slope in both equations, and  $\sigma$  denotes the intercept standard deviation. The calculated LOD and LOQ were  $4.0$  and  $14.0 \text{ ng mL}^{-1}$ , respectively.

The proposed electrode was compared with that of the previously reported electrodes, as presented in Table 3. The developed electrode provided the best LOD compared to the other electrodes used in the published methods.

### 3.5.3. Accuracy and precision

Three different LNG concentrations were used to assess the method's accuracy, and the result was given as a percent recovery (Table 4). The analysis indicated that the technique is highly accurate as the obtained percent recovery was nearly 100%.

Precision was examined at inter-day and intra-day levels by analyzing three different concentrations of LNG standard

solution in triplicates. The replicated study was performed on the same day for the intra-day level, while in the case of the inter-day level, the study was done on three successive days. A summary of the analysis is presented in Table 5. The obtained RSD was below 2.0% at the two levels, verifying the high degree of precision at the two levels.

### 3.5.4. Selectivity

The voltammetric measurements were conducted for the determination of a fixed concentration of the drug alone. Then analysis was repeated in the existence of some interfering substances. The interference study involved the following: copper sulphate, magnesium stearate, thiourea, ascorbic acid, citric acid, dextrose, lactose, starch, cellulose, in addition to the co-formulated drug, metformin. These components were added at ten times the LNG concentration. It was observed that no significant matrix interference was encountered in LNG determination by these substances as the found recoveries percent ranged from 97.37 to 104.91% (Table 6). So, the proposed approach for determining LNG has high selectivity.

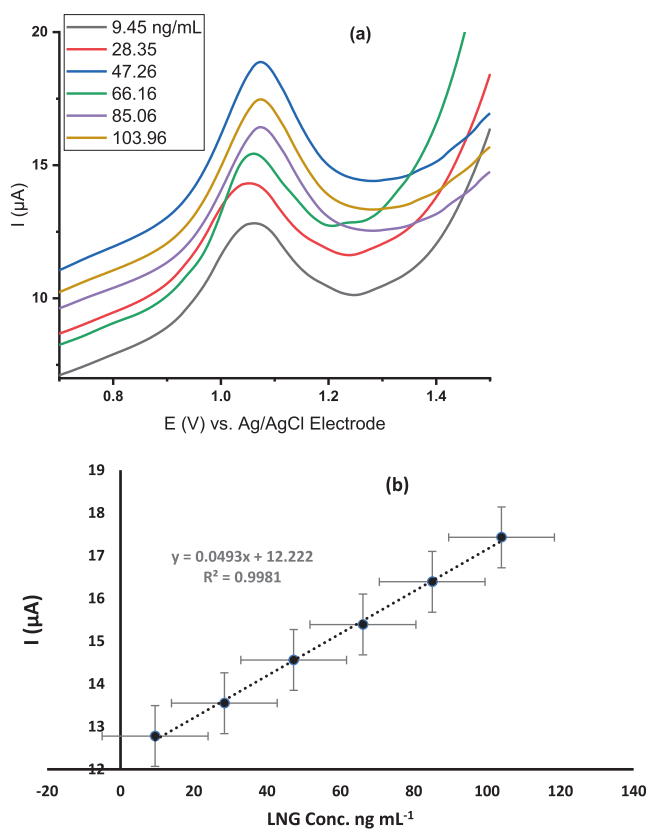


**Fig. 11** The voltammograms (a) and the peak current calibration curve (b) against different LNG concentrations ( $\text{ng mL}^{-1}$ ) using GO-GCE. Conditions; 0.04 M phosphate buffer (pH 6.5), accumulation potential + 0.6, and accumulation time 480 s.

**Table 2** Regression data for the determination of LNG at Go-GCE SWAdASV method.

Parameter	Value
Linear range ( $\text{ng mL}^{-1}$ )	9.45–103.96
Slope	0.0493
The standard deviation of slope	0.0011
Intercept	12.22
The standard deviation of the intercept	0.071
Correlation coefficient ( $r$ )	0.9981
The standard deviation of the residuals	15.19
LOD $\text{ng mL}^{-1}$	4.0
LOQ $\text{ng mL}^{-1}$	14.0

The number of experiments,  $n = 6$ .

### 3.6. Application of the proposed method

#### 3.6.1. Analysis of tablet dosage form

The proposed method was able to analyze Trajenta® tablets containing LNG. The mean recovery value was 99.80%, with an SD of 1.19. These results were compared with those of the published method (Aher et al., 2017) at a 95% confidence level, as shown in Table 7. There is no notable discrepancy in the accuracy and precision of both methods as the calculated

**Table 3** Comparison of the proposed electrode with previously reported electrodes to the determination of LNG by square wave voltammetric technique.

Electrode	LOD ( $\text{ng mL}^{-1}$ )	Ref.
GO-GCE	4.00	This work
$\text{Co}_3\text{O}_4$ NPs, MWCNTs-CPE	5340.00	(Elshahed et al., 2020)
PGE	100.00	(Naggar et al., 2020)
Cu-PGE	6.23	(Gahlan, 2021)
GCE	52.00	(Gahlan, 2021)
L-cysteine, $\text{MoS}_2$ -GCE	89.78	(Ateş et al., 2021)
$\text{Fe}_2\text{O}_3$ -CPE	8.00	(El-Shal et al., 2019)
GCE- E-rGO/Poly (B-CD)/magnetic ZIF-67	5.0	(Baezzat and Shojaei, 2021)

**Table 4** Accuracy of determination of LNG by the proposed method.

Conc. taken from LNG ( $\text{ng mL}^{-1}$ )	Con. found of LNG ( $\text{ng mL}^{-1}$ )	Recovery* % $\pm$ SD	RSD
28.35	27.75	97.88 $\pm$ 1.01	1.03
66.15	66.19	100.60 $\pm$ 1.52	1.51
85.06	87.14	102.44 $\pm$ 1.10	1.08

\* Mean of five determinations.

**Table 5** Evaluation of the intra- and inter-day precisions of the proposed method for the determination of the LNG at three concentrations.

Precision level	Conc. Level ( $\text{ng mL}^{-1}$ )	Conc. found ( $\text{ng mL}^{-1}$ )	% Recovery* $\pm$ SD	RSD
Intra-day	28.35	28.85	101.76 $\pm$ 1.52	1.49
	66.15	65.86	99.56 $\pm$ 1.21	1.22
	85.06	82.01	96.42 $\pm$ 1.08	1.12
Inter-day	28.35	28.88	101.86 $\pm$ 1.67	1.64
	66.15	65.71	99.34 $\pm$ 1.52	1.53
	85.06	81.88	96.26 $\pm$ 1.30	1.35

\* Mean of five determinations.

values of the t- and F-tests did not exceed the theoretical values.

#### 3.6.2. Analysis of spiked plasma and urine

Different quantities of LNG were added to plasma and urine samples, and the proposed method was applied to these spiked samples. The calibration curves were constructed for both plasma and urine samples. The obtained linear regression equations were  $I_p = 0.0433C + 12.26$  ( $R^2 = 0.9980$ ) with an SD of 1.23 for spiked plasma and  $I_p = 0.0464 + 12.02$  ( $R^2 = 0.9979$ ) with an SD of 1.56 for spiked urine, where  $I_p$  is the peak current in  $\mu\text{A}$ , and  $C$  is the drug concentration in  $\text{ng mL}^{-1}$ . Three different samples of spiked plasma and urine were analyzed, and their drug contents were estimated using

**Table 6** Effect of the interfering substances on the determination of 96.95 ng mL<sup>-1</sup> of LNG using the proposed SWAdASV technique with GCE-GO.

Interferent	Conc. Found (ng mL <sup>-1</sup> )	Recovery (%)	± SD
CuSO <sub>4</sub>	94.68	97.66	1.66
Thiourea	95.74	98.75	0.88
Ascorbic acid	94.40	97.37	1.86
Citric acid	98.53	101.63	1.15
Dextrose	99.49	102.62	1.85
Metformin	101.71	104.91	3.47
Cellulose	100.15	103.30	2.34
Starch	98.04	101.12	0.79
Magnesium stearate	99.40	102.53	1.79
Lactose	100.00	103.15	2.23

\*Mean of three determinations.

**Table 7** Application of the proposed method for the analysis of Trajenta® tablets (5 mg of LNG per pill) by both the proposed and the reported methods (Gopalan et al., 2007).

Parameters	Reported method	Proposed method
% Recovery <sup>a</sup>	100.07	99.80
± SD	1.09	1.19
t-value <sup>b</sup>	–	0.25
F-value <sup>b</sup>	–	1.19

<sup>a</sup> The value is the mean of five determinations for both methods.<sup>b</sup> Tabulated values at 95% confidence limit are  $t = 2.306$ ,  $F = 6.338$ .

the previous regression equations. The results presented in Table 8 show that the percent recoveries ranged from 88.79 to 94.12% in spiked plasma and urine. These promising results indicated that the proposed method could detect LNG with a little plasma and urine matrix effect.

**Table 8** Results of using the proposed method to determine the LNG in spiked plasma and urine.

LNG conc. (ng mL <sup>-1</sup> )	Drug. Found (ng mL <sup>-1</sup> )	Recovery* % ± SD	RSD
<b>Spiked plasma</b>			
28.35	25.78	90.95 ± 1.08	1.19
47.25	42.18	89.26 ± 1.29	1.44
85.06	75.52	88.79 ± 1.31	1.48
<b>Spiked urine</b>			
28.35	26.21	92.45 ± 1.64	1.77
47.25	44.47	94.12 ± 1.31	1.39
85.06	79.74	93.63 ± 1.73	1.84

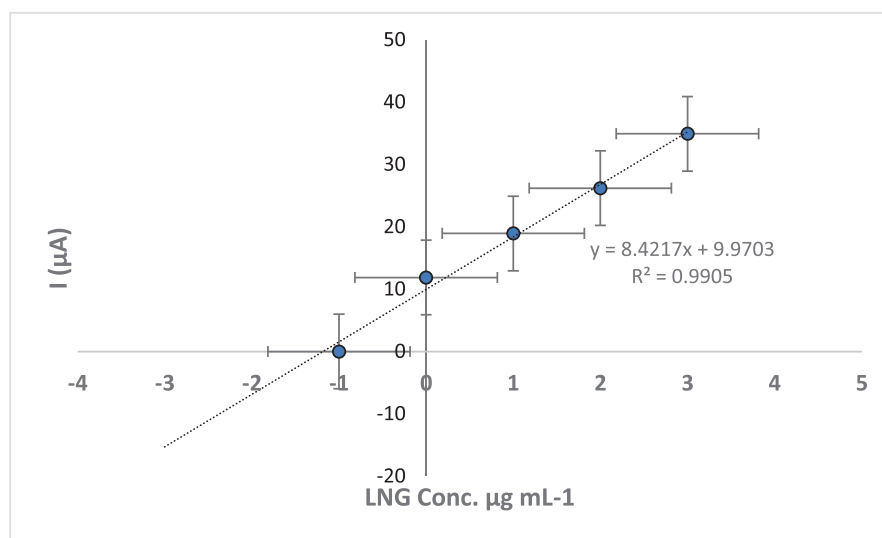
\* Mean of three determinations.

### 3.6.3. Analysis of rats' feces

It is reported that LNG is excreted mainly via feces, so it is essential to employ the developed method to determine its presence in the feces. Therefore, the standard addition method (Fig. 12) was used to determine the unknown concentration of LNG in the feces sample. First, a supernatant feces sample and three concentrations of standard LNG solution were used. The main recovery was 97.09%, with an SD of 2.31. This value indicated that the method was suitable to determine LNG in the feces sample.

## 4. Conclusion

A glassy carbon electrode was modified with graphene oxide, and the electrode surface was characterized with SEM, FTIR, and XRD. Investigating the electrochemical behavior of LNG on the prepared electrode with cyclic voltammetry revealed that the drug was irreversibly oxidized through a single electron and proton transfer. The modified electrode was employed to analyze the drug using square wave anodic

**Fig. 12** Calibration graph for direct determination of LNG in rats' feces sample using standard addition method.

adsorptive stripping voltammetry. The method was accurate, precise, and had low detection and quantitation limits. The modified electrode's proposed voltammetric technique has the lowest detection limit compared to the previously reported electrodes. The method was efficiently used in the analysis of LNG in its pharmaceutical tablets, spiked human fluids, and first in the rats' feces.

## References

- Bjørnar, A.D., G. Hilary, K. Pierre, L. Jean-Claude, M. Martin, S. Linda, S. Rhys, W. Paul, Z., 2015. Diabetes Atlas. In: INT. Diabetes Fed., International Diabetes Federation: Brussels, Belgium. p. 297.
- Godman, B., Basu, D., Pillay, Y., Mwita, J.C., Rwegerera, G.M., Anand Paramadhas, B.D., Tiroyakgosi, C., Okwen, P.M., Niba, L. L., Nonvignon, J., 2020. Review of ongoing activities and challenges to improve the care of patients with type 2 diabetes across Africa and the implications for the future. *Front. Pharmacol.* 11, 1–21.
- Deacon, C.F., 2018. A review of dipeptidyl peptidase-4 inhibitors. Hot topics from randomized controlled trials. *Diabetes Obes. Metab.* 20, 34–46.
- Deeks, E.D., 2012. Linagliptin: a review of its use in the management of type 2 diabetes mellitus. *Drugs* 72 (13), 1793–1824.
- Rizk, M. et al, 2020. Development and validation of thin-layer chromatography and high-performance thin-layer chromatography methods for the simultaneous determination of linagliptin and empagliflozin in their co-formulated dosage form. *JPC-J. Planar Chromat.* 33 (6), 647–661.
- Patil, C.V.P., Patil, P.A., 2020. Development of Validation of Zero order, First-order, Second-order, UV-Spectrophotometry Methods using AUC Technique for Quantitative Estimation of Linagliptin in Bulk Material and Tablets. *Asian J. Res. Chem.* 13 (3), 228–232.
- Aref, H.A., Haammad, S.F., Elgawish, M.S., Darwish, K.M., 2020. A Determination of Novel Promising Combination of Linagliptin and Pioglitazone HCl in Bulk and Laboratory Synthetic Mixture by Earth-Friendly Three Spectrophotometric Methods. *Rec. Pharm. Biomed. Sci.* 4 (2), 1–12.
- Vijayalakshmi, R., Naveena, V.S., 2019. Approach of Spectrophotometric Methods for Quantitative Estimation of Jenadueto Tablets. *Asian J. Biochem. Pharm. Res.* 9 (2), 38–44.
- El-Bagary, R.I.E., Elkady, E.F., Ayoub, B.M., 2014. Spectrofluorometric determination of linagliptin in bulk and in pharmaceutical dosage form. *Eur. J. Chem.* 5 (2), 380–382.
- Aref, H.A., Hammad, S.F., Elgawish, M.S., Darwish, K.M., 2020. Novel spectrofluorimetric quantification of linagliptin in biological fluids exploiting its interaction with 4-chloro-7-nitrobenzofurazan. *Luminescence* 35 (5), 626–635.
- Omar, M.A., Haredy, A.M., Saleh, G.A., Naggar, A.H., Derayea, S. M., 2019. Diarylpyrrolone based fluorophore for the selective spectrofluorometric method for determination of Linagliptin antidiabetic drug in pharmaceutical tablets. *Microchemical J.* 148, 555–560.
- Elmasry, M.S. et al, 2021. Fluorimetric study on antidiabetic combined drugs; empagliflozin and linagliptin in their pharmaceutical formulation and human plasma. *J. Spectrochimica Acta Part A: Mol. Biomol. Spectrosc.* 248, 119258.
- Patel, I.M. et al, 2020. Densitometric simultaneous estimation of combination of empagliflozin, linagliptin and metformin hydrochloride used in the treatment of type 2 diabetes mellitus. *JPC-J. Planar Chromat* 33 (2), 109–118.
- Bhole, R. et al, 2017. High performance thin layer chromatographic determination of linagliptin in pharmaceutical formulations and in biological samples. *Int. J. Pharma. Chem. Anal.* 4 (4), 13–19.
- Bhole, R.P., Wankhede, S.B., Zambare, Y.B., Wankhede, T.S., 2017. High performance thin layer chromatographic determination of linagliptin in pharmaceutical formulations and in biological samples. *Int. J. Pharma. Chem. Anal.* 4 (1), 13–19.
- Sivagami, B.P., Purushotham, A., Sikdar, P., Chandrasekar, R., Babu, M.N., 2020. A Validated Method for The Simultaneous Estimation of Linagliptin and Metformin in Tablet Dosage Forms by RP-HPLC. *Res. J. Pharm. Technol.* 13 (3), 1266–1270.
- Raut, A.N., Jawarkar, G.S., Khodke, S.V., Khole, A.V., 2020. Method development, validation by simultaneous estimation of empagliflozin and linagliptin by RP-HPLC method. *J. Pharm. Sci. Innovation* 9 (1), 1–4.
- Kiran, T.N.R., Parvathi, P., Kumar, J.S., 2020. Development and validation of rp-hplc method for the simultaneous estimation of linagliptin, empagliflozin and metformin in solid dosage forms. *Asian J. Pharm. Anal. Med. Chem.* 10 (3), 117–124.
- Al-Bratty, M.M., Murayzin, H., Tawhari, Almanaa A., Rehman, M.Q., Alhazmi, Z.U., Javed, H.A., Alam, S.A., Md, S., 2019. Quantitative Conductometric Determination of Sitagliptin, Linagliptin, Vildagliptin and Alogliptin by Applying the Concept of Drug-Metal ion Interaction. *Orient. J. Chem.* 35 (5), 1597–1604.
- Elshahed, M.R., Elshahed, M.S., Attia, A.K., Mohamed, H.Y., 2020. Validated Voltammetric Method for the Simultaneous Determination of Anti-diabetic Drugs, Linagliptin and Empagliflozin in Bulk, Pharmaceutical Dosage Forms and Biological Fluids. *Electroanalysis* 32, 1–18.
- Naggar, A.H.S., Saleh, G.A., Omar, M.A., Haredy, A.M., Derayea, S. M., 2020. Square Wave Adsorptive Anodic Stripping Voltammetric Determination of Antidiabetic Drug Linagliptin in Pharmaceutical Formulations and Biological Fluids Using Pencil Graphite Electrode. *J. Anal. Sci.* 36 (9), 1031–1038.
- Gahlan, A.A. et al, 2021. Square Wave Anodic Voltammetric Determination of Antidiabetic Drug Linagliptin in The Dosage Form and Biological Fluids by Microparticles Copper Pencil Graphite Electrode. *Egyptian J. Chem.* 64 (6), 3121–3130.
- Ateş, A.K., Çelikkhan, H., Erk, N., 2021. Voltammetric determination of linagliptin in bulk and plasma sample using an electrochemical sensor based on L-cysteine modified 1T-MoS<sub>2</sub> nanosheets. *Microchem. J.* 167, 106308.
- Gahlan, A.A. et al, 2021. A Glassy Carbon Electrode for the Determination of Linagliptin, an Antidiabetic Drug in Pure Form, Tablets and Some Biological Fluids by Adsorptive Stripping Voltammetry. *Curr. Pharm. Des.* 27 (10), 2415–2424.
- El-Shal, M.A.A., Azab, S.M., Hendawy, H.A.M., 2019. A facile nano-iron oxide sensor for the electrochemical detection of the antidiabetic drug linagliptin in the presence of glucose and metformin. *Bull. Natl. Res. Cent. (Egypt)* 43 (1), 95–103.
- Baezzat, M.R., Shojaei, F., 2021. Electrochemical sensor based on GCE modified with E-rGO/Poly (B-CD)/magnetic ZIF-67 nanocomposite for the measurement of Linagliptin. *Diam. Relat. Mater.* 114, 108345.
- Yang, C.D., Denno, M.E., Pyakurel, P., Venton, B.J., 2015. Recent trends in carbon nanomaterial-based electrochemical sensors for biomolecules: A review. *Anal. Chim. Acta* 887, 17–37.
- Mirceski, V., Gulaboski, R., Lovric, M., Bogeski, I., Kappl, R., Hoth, M., 2013. Square-wave voltammetry: A review on the recent progress. *J. Electroanal.* 25 (11), 2411–2422.
- Shigemitsu, T., Matsumoto, G., Tsukahara, S., 1979. Electrical properties of glassy-carbon electrodes. *J. Med. Biol. Eng. Comput.* 17 (4), 465–470.
- Marcano, D.C. et al, 2010. Improved synthesis of graphene oxide. *J. ACS Nano* 4 (8), 4806–4814.
- Kariper, İ.A., Çağlayan, M.O., Üstündağ, Z., 2019. Heterogeneous Au/Ru hybrid nanoparticle decorated graphene oxide nanosheet catalyst for the catalytic reduction of nitroaromatics. *Res. Chem. Intermed.* 45 (2), 801–813.

- Korkmaz, S., Kariper, İ.A., 2020. Graphene and graphene oxide based aerogels: Synthesis, characteristics and supercapacitor applications. *J. Energy Storage* 27, 101038.
- Karthik, R. et al, 2017. A facile graphene oxide based sensor for electrochemical detection of prostate anti-cancer (anti-testosterone) drug flutamide in biological samples. *J. RSC Adv.* 7 (41), 25702–25709.
- Vadivaambigai, A. et al, 2015. Graphene-oxide-based electrochemical sensor for salicylic acid. *Nanosci. Nanotechnol. Lett.* 7 (2), 140–146.
- Zidan, M. et al, 2014. Electrochemical detection of paracetamol using graphene oxide-modified glassy carbon electrode. *Int. J. Electrochem. Sci.* 9, 7605–7613.
- Canbay, E.T., Türkmen, H., Akyilmaz, E., 2014. Ionic liquid modified carbon paste electrode and investigation of its electrocatalytic activity to hydrogen peroxide. *Bull. Mater. Sci.* 37 (3), 617–622.
- Hummers, J.W.S.O., Offeman, R.E., 1958. Preparation of graphitic oxide. *J. Am. Chem. Soc.* 80 (6), 1339.
- Chaiyakun, S.W., Witit-Anun, N., Nuntawong, N., Chindaudom, P., Oaew, S., Kedkeaw, C., Limsuwan, P., 2012. Preparation and characterization of graphene oxide nanosheets. *Procedia Eng.* 32, 759–764.
- Bahrami, A.K., Kazeminezhad, I., Abdi, Y., 2019. Pt-Ni/rGO counter electrode: electrocatalytic activity for dye-sensitized solar cell. *Superlattices Microstruct.* 125, 125–137.
- Albayrak, İ. et al, 2017. Isophthalic acid terminated graphene oxide modified glassy carbon nanosensor electrode: Cd<sup>2+</sup> and Bi<sup>3+</sup> analysis in tap water and milk samples. *Int. J. Food Prop.* 20 (7), 1558–1568.
- Prashanth, S.N.R., Ramesh, K.C., Seetharamappa, J., 2011. Electrochemical oxidation of an immunosuppressant, mycophenolate mofetil, and its assay in pharmaceutical formulations. *Int. J. Electrochem.* 2011, 1–7.
- Laviron, E., 1979. General expression of the linear potential sweep voltammogram in the case of diffusionless electrochemical systems. *J. Electroanal. Chem. Interfacial Electrochem.* 101 (1), 19–28.
- Kim, D.-K. et al, 2010. Effect of ionic mobility of working electrolyte on electrokinetic energy conversion in sub-micron channels. *Int. J. Therm. Sci.* 49 (7), 1128–1132.
- Gowda, J.I., Nandibewoor, S.T., 2014. Electrochemical behavior of paclitaxel and its determination at glassy carbon electrode. *Asian J. Pharm. Sci. (Amsterdam, Neth.)* 9 (1), 42–49.
- Allen, J.B., Larry, R.F., 2001. *Electrochemical methods fundamentals and applications.* John Wiley & Sons.
- Gopalan, A.I.L., Lee, K.P., Manesh, K.M., Santhosh, P., Kim, J.H., Kang, J.S., 2007. Electrochemical determination of dopamine and ascorbic acid at a novel gold nanoparticles distributed poly (4-aminothiophenol) modified electrode. *Talanta* 71 (4), 1774–1781.
- Scholz, F., 2015. *Voltammetric techniques of analysis: the essentials.* ChemTexts 1 (4), 1–24.
- Teófilo, R.F., Reis, E.L., Reis, C., Silva, G.A.D., Kubota, L.T., 2004. Experimental design employed to square wave voltammetry response optimization for the glyphosate determination. *J. Braz. Chem. Soc.* 15 (6), 865–871.
- Validation of analytical procedures: text and methodology Q2 (R1). In: *International Conference on Harmonization.* 2005. Geneva, Switzerland.
- Aher, S.S., Gajare, S., Saudagar, R.B., 2017. Spectrophotometric and Chromatographic Estimation of Linagliptin in Bulk and Tablet Dosage Form. *Int. J. ChmTech Res.* 10 (6), 736–744.